# Observer design for Lightweight Robotic arm actuated by Shape Memory Alloy (SMA) wire

Serket Quintanar-Guzmán
*SnT*
*University of Luxembourg*
Luxembourg, G. D. of Luxembourg
serket.quintanar@uni.lu

Somasundar Kannan
*SnT*
*University of Luxembourg*
Luxembourg, G. D. of Luxembourg
somasundar.kannan@uni.lu

Holger Voos
*SnT*
*University of Luxembourg*
Luxembourg, G. D. of Luxembourg
holger.voos@uni.lu

Mohamed Darouach
*UHP Nancy I IUT de Longwy*
*Centre de Recherche en*
*Automatique de Nancy*
Cosnes-et-Romai, France
modar@pt.lu

Marouane Alma
*UHP Nancy I IUT de Longwy*
*Centre de Recherche en*
*Automatique de Nancy*
Cosnes-et-Romai, France
marouane.alma@univ-lorraine.fr

***Abstract*—This paper presents the design of an observer for a lightweight robotic arm actuated by a single biased Shape Memory Alloy (SMA) wire. The internal states of the system are estimated via an Extended Kalman Filter (EKF) with sliding mode unknown input and states estimation. This observer allows estimating the temperature, stress and martensite fraction rate of the SMA wire. This approach avoids the use of switching dynamics in the observer's model, due to the martensite fraction being considered as the unknown input. The discretized model of the robotic arm and observer development is presented. Finally the effectiveness of the proposed observer is tested in simulation.**

***Index Terms*—EKF, Unknown Input, SMA wire, robotic arm, lightweight, sliding mode**

## I. Introduction

Shape Memory Alloys (SMA) are a group of metallic materials with Shape Memory Effect(SME). This characteristic gives them the ability to recover their original shape after mechanical deformantion. For this effect to take place certain type of stimuli must be applied, such as thermal variations.There are different types of SMA materials, the most common one being the Nickle-Titanium alloy commonly know as Nitinol [1].

These materials have numerous characteristics that have made them a great substitute to conventional actuators. Among these characteristics are the following: noiseless operation, bio-compatibility, high mass-force ratio, magnetic susceptibility, damping and more. Due to these characteristics, SMA has been commonly used to develop actuators in recent years [2]. Among these we can find medical applications such as intra-arterial supports [3], aerodynamic applications such as actuator for morphing segments on a UAV wing [4]. More general applications can also be found as in [5] where the authors propose a SMA actuated car mirror or [6] where a SMA based motor is designed. In addition, this material has been used in the robotic field for the development of robotic manipulator like the lightweight robotic arm presented in [7].

In spite of the great characteristics of this smart materials, they also have disadvantages which represent a great challenge in the aspect of control. SMAs have highly nonlinear dynamics due to a phenomena known as hysteresis. This type of nonlinear behavior greatly hampers the development of accurate control. Although they possess Hysteresis behavior, SMA wires have linear relation between its internal states, for example Resistance-Strain or Martinsite fraction-Strain [8]. However, the internal states of SMAs often are immeasurable in real applications or require complex equipment to do so. A solution to this problem is the estimation of the internal states, so the purpose of the article is to discuss suitable observer design.

When talking about estimation for SMA wires, the research found in the literature is limited and mostly concentrated on the estimation of the mechanical states of SMA based actuators. A Luenberger observer for the estimation of the mechanical states (position and velocity) were proposed in [9] and [10]. In [11] an Extended Kalman Filter (EKF) was applied to predict the state of the SMA based system while an Artificial Neural Network (ANN) has been used to compensate for the inaccuracies caused by the dynamic of the biased spring. In [12] the authors present an augmented EKF for the estimation of temperature, stress and spring parameters, based on a deterministic SMA switching model while the stability of the system is barely mentioned. Finally the authors in [13] present a disturbance observer for an SMA actuated smart joint.

Most of these approaches demand complex switching models or intelligent control using ANN. With this in mind, we propose a new approach for the estimation of SMA's internal states, including the martensite fraction. We propose an Extended Kalman Filter with sliding mode for unknown

input and states estimation for a SMA wire actuated robotic arm. This approach allows the estimation of the SMA wire states avoiding the switching inside the observer's model. Furthermore, it is capable to estimate the martensite fraction rate, which as already mention is a critical parameter for modeling the SMA wire dynamic and an interesting alternative to control design.

The current paper is organized as follows: First the mechanical design and mathematical model of a lightweight SMA actuated robotic arm is presented in Section II. In Section III the proposed Extended Kalman Filter observer incorporating sliding mode for estimation of the martensite fraction rate (unknown input) is described, while Section IV presents the estimation of the unknown input through the sliding mode. In Section V the Extended Kalman Filter with Unknown Input (EKF-UI) observer is applied for estimation of the states and unknown input of a SMA wire actuated robotic arm, while the simulation results are shown in Section VI. Finally the conclusions are presented in Section VII.

## II. SMA ACTUATED ROBOTIC ARM

Nowadays aerial manipulation has became a trend topic in the robotics field. When dealing with aerial manipulation with small Unnamed Aerial Vehicles (UAV), the optimal use of the available payload is a critical point. Addressing this problem, we propose a lightweight robotic arm actuated by SMA wires previously published in [7] and [14]. This design proposes a SMA actuated single degree of freedom Robotic Arm which weighs a total of 48 g. Figure 1 shows a Computer Aided Design (CAD) of the proposed robotic arm. This design is based on the joint proposed in [15]. This joint consist of two couplers fixed together by a torsion spring and actuated by a single SMA wire. The proposed observer will be tested over the biased wire configuration, where the Wire-2 is a rigid wire. So in this configuration only 1 SMA will be actuated and the biased force will be provided by a torsion spring (for further details on the design please refer to [7] or [14]).

### A. Robotic arm model

The model of the robotic arm can be divided into three submodels: 1) SMA wire model, 2) Kinematic model and 3) Dynamics. Figure 2 shows the block diagram of the complete system.

*1) SMA wire model.:* The model of the SMA wire, is further subdivided into three recursive models. The heat transfer model describes the dynamic of a system heated by joule effect and cooled by natural convection where the convection coefficient is approximated by a second order polynomial of the temperature.

The SMA wire phase transformation model computes the martensite fraction rate ($\dot{\xi}$). This parameter depends on the temperature and stress of the SMA. It is a highly nonlinear switching dynamic parameter, which is responsable for the typical hysteretic behavior of the SMA wires. Two equations are needed to fully describe the full hysteresis major and minor loops, one while heating and the second for cooling.

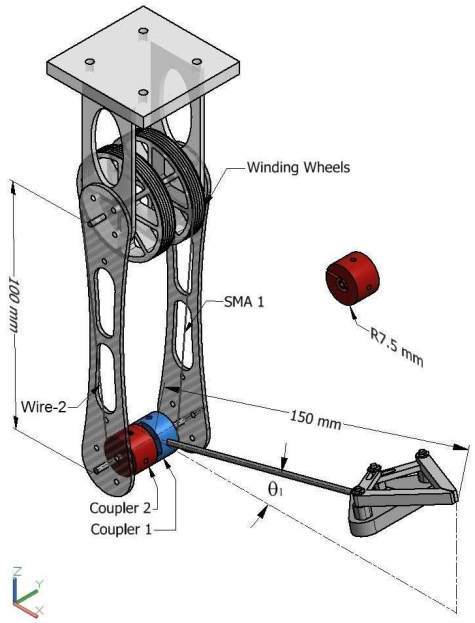


Fig. 1. Proposed SMA wire actuated robotic arm CAD model.

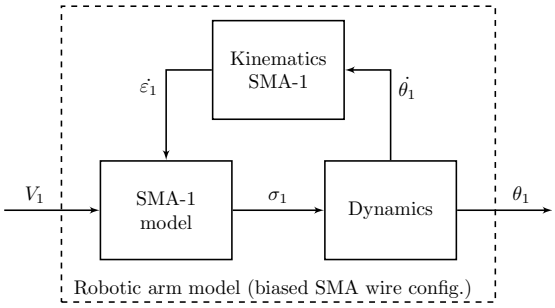


Fig. 2. Block diagram of the SMA actuated robotic arm.

The wire constitutive model describes the relation between the SMA wire dynamic states and the mechanical effect caused by the same wire (defined by Stress ($\sigma$)). This model was presented by [16] and then modified by [17]:

$$\dot{\sigma} = E\dot{\varepsilon} + \Omega\dot{\xi} + \Theta\dot{T}, \tag{1}$$

where $\Omega$ and $\Theta$ are the phase transformation constant and thermal expansion coefficient, respectively. We have $\Omega = -E\varepsilon_0$ and $\varepsilon_0$ is the initial strain.

*2) Kinematic model.:* This model relates the SMA wire model with the mechanics of the robotic arm itself. The strain ratio of the SMA wire and angular velocity of the arm depends on the geometry of the design.

*3) Dynamic model.:* The dynamic system gives the relation between the SMA wire actuation and the mechanical effects over the end-effector. The general dynamic model of the mechanical system is described as:

$$M(\theta)\ddot{\theta} + V_m\left(\theta, \dot{\theta}\right)\dot{\theta} + g(\theta) + F_d\dot{\theta} + \Phi(\theta, \theta_r) = \tau_\omega \tag{2}$$

where $\theta, \dot{\theta}, \ddot{\theta}$ represent the positions, velocities and accelerations of the couplers, $M(\theta)$ is the inertia matrix, $V_m\left(\theta, \dot{\theta}\right)$ is the centripetal-coriolis matrix, $g(\theta)$ is considered as the effect of gravity, $F_d$ is the viscous coefficient term, $\Phi(\theta, \theta_r)$ is the nonlinear hysteretic term, $\tau_\omega$ is the input torque applied to the manipulator joint by the SMA wire, which is mathematically described as:

$$\tau_w = F_w r = A\sigma r \tag{3}$$

For further details on the full SMA wire actuated robotic arm model and design, please refer to [18].

## III. Extended Kalman Filter with Unknown Input

In this section the observer structure and characteristics of the system are defined. Consider the following discrete nonlinear system:

$$\begin{aligned} x_{k+1} &= f(x_k, u_k, r_k) + \phi(x_k)\, d(x_k, u_k) \\ y_k &= h(x_k, w_k) \end{aligned} \tag{4}$$

where $x_k = [x_{1k}, x_{2k}, ..., x_{nk}]^T \in \mathbb{R}^n$ is the state vector at instant $k$, $u_k \in \mathbb{R}^r$ and $y_k \in \mathbb{R}^p$ are the input and output vectors at time instant $k$, $d(x_k, u_k)$ is the unknown input and $\phi(x_k)$ is the distribution matrix of unknown inputs,$r_k$ is the system noise cause by the parameter inaccuracies and $w_k$ is the measurement noise. Both, system and measurement noise matrices are modeled as Gaussian noises with zero mean and completely independent.

Assuming the function $f(x_k, u_k)$ is bounded with respect to its own arguments and system 4 is uniformly observable while the unknown input is also bounded as $|d(\cdot)| \leq \overline{d}$. The Extended Kalman Filter with Unknown Input (EKF-UI) observer is proposed as follows:

1) Measurement update

$$\begin{aligned} \hat{x}_{k+1} &= \hat{x}_{k+1/k} + K_{k+1} e_{k+1} \\ K_{k+1} &= P_{k+1/k} H_{k+1}^T \left(H_{k+1} P_{k+1/k} H_{k+1}^T + R_{k+1}\right)^{-1} \\ P_{k+1} &= \left(I - K_{k+1} H_{k+1}\right) P_{k+1/k} \end{aligned} \tag{5}$$

2) Time update

$$\begin{aligned} \hat{x}_{k+1/k} &= f(\hat{x}_k, u_k) + \phi(\hat{x}_k)\, \hat{d}(x_k, u_k) \\ P_{k+1}/k &= F_k P_k F_k^T + Q_k \end{aligned} \tag{6}$$

Where

$$e_{k+1} = y_{k+1} - h\left(\hat{x}_{k+1/k}, w_{k+1}\right) \tag{7}$$

$$F_k = f(\hat{x}_k, u_k) = \left.\frac{\partial f(x_k, u_k)}{\partial x_k}\right|_{\hat{x}_k = \hat{x}_k} \tag{8}$$

$$H_{k+1} = H\left(\hat{x}_{k+1/k}\right) = \left.\frac{\partial h(x_{k+1}, w_{k+1})}{\partial x_{k+1}}\right|_{\hat{x}_{k+1} = \hat{x}_{k+1/k}} \tag{9}$$

here $Q_k$ and $R_k$ are diagonal matrices, which represent the covariance matrices of the system ($r_k$) and measurement ($w_k$) noises respectively. These matrices satisfy:

$$\begin{cases} Q = cov(r) = E\left[rr^T\right] \\ R = cov(w) = E\left[ww^T\right] \end{cases} \tag{10}$$

Different methods can be used to estimate the unknown input, but in the current article we will consider the Unknown Input Estimator based on Sliding Modes which is presented next.

## IV. Sliding Mode Unknown input estimation

This approach is based on the work presented in [19], where a high-gain observer with sliding mode for state and unknown input estimations is developed with stability discussion. Using this approach the unknown input can be estimated using a sliding surface defined as a function of the first term of the estimation error ($e_{1k}$) as follows [19]:

$$\hat{d}(x_k, u_k) = -\rho sign(e_{1k}) \tag{11}$$

where $\rho$ is the sliding mode gain.

To avoid the chattering caused by the $sign(\cdot)$ function (characteric challenge of sliding mode technique), this fuction is replaced by a $sat(\cdot, \epsilon)$, defined as [20]:

$$sat(\cdot, \epsilon) = \begin{cases} \cdot/\epsilon, & \text{if } |\cdot| \leq \epsilon, \\ sign(\cdot), & \text{if } |\cdot| > \epsilon. \end{cases} \tag{12}$$

## V. Application to SMA wire based robotic arm

The martensite fraction rate, necessary for the estimation of the stress via the constitutive model of the SMA wire, is a switching nonlinear parameter of the SMA wire. The explicit estimation of this parameter demands switching dynamics inside the observer, which can lead to instability. For this reason, a new approach is presented, where the martensite fraction rate is considered as an unknown input or disturbance to the system ($d(x_k, u_k)$). Using this method we avoid the necessity of a switching dynamic in the estimation model. Let us define the discretized model of the SMA actuated robotic arm with martensite fraction as the unknown input in the following way:

$$\begin{aligned} f(x_k, u_k) = &\begin{bmatrix} x_{1k} \\ x_{2k} \\ x_{3k} \\ x_{4k} \end{bmatrix} + \\ &\begin{bmatrix} x_{2k} \\ \frac{A_1 r_1}{J_1} x_{4k} - \frac{b_1}{J_1} x_{2k} - \frac{m_{load} g r_{load}}{J_1} \cos(x_{1k}) - \\ \frac{1}{R_1 m_{w_1} c_{p_1}} V_k^2 - \\ -\frac{Er}{l_0} x_{2k} \end{bmatrix} \\ &\begin{bmatrix} 0 \\ \frac{1}{J_1}\tau_s(x_{1k}, x_{2k}) \\ \frac{h_1 A_{w_1}}{m_{w_1} c_{p_1}}(x_{3k} - T_{amb}) \\ +\Theta\left(\frac{1}{R_1 m_{w_1} c_{p_1}} V_k^2 - \frac{h_1 A_{w_1}}{m_{w_1} c_{p_1}}(x_{3k} - T_{amb})\right) \end{bmatrix} T_s \end{aligned} \tag{13}$$

$$\phi\left(x_k, u_k\right) = \begin{bmatrix} 0 \\ 0 \\ 0 \\ -\Omega T_s \end{bmatrix} \tag{14}$$

$$d\left(x_k, u_k\right) = \begin{bmatrix} 0 \\ 0 \\ 0 \\ \dot{\xi}_k \end{bmatrix} \tag{15}$$

$$h\left(x_k, w_k\right) = \begin{bmatrix} x_{1k} \\ x_{2k} \end{bmatrix} + w_k \tag{16}$$

Further the state vector is defined as follows:

$x_{1k}$ - Angular position of coupler-1 $(\theta_1)$

$x_{2k}$ - Angular velocity of coupler-1 $\left(\dot{\theta}_1\right)$

$x_{3k}$ - Temperature of SMA wire-1 $(T_1)$

$x_{4k}$ - Stress of SMA wire-1 $(\sigma_1)$

It is important to mention that the only measurable state in this system is the position of coupler-1 ($x_{1k}$), while the angular velocity of the coupler-1 ($x_{2k}$) can be computed from this measurement. So the temperature and stress of the wire are estimated. In order to apply the proposed EKF-UI algorithm (Equations 5 - 9) let us define the required state and output matrices as follows:

$$F_k = \begin{bmatrix} 1 & T_s & 0 & 0 \\ \frac{T_s}{J_1}\left[-k_s + k_1 \sin\left(x_{k1}\right)\right] & 1 - \frac{T_s}{J_1}\left(b_s + b_1\right) & 0 & \frac{T_s r A_w}{J_1} \\ 0 & 0 & 1 - \frac{h_1 A_{w_1}}{m_{w_1} c_{p_1}} T_s & 0 \\ 0 & -\frac{Er}{l_0} T_s & \Theta\left(1 - \frac{h_1 A_{w_1}}{m_{w_1} c_{p_1}} T_s\right) T_s & 1 \end{bmatrix} \tag{17}$$

$$H_k = \begin{bmatrix} 1 & 0 & 0 & 0 \\ 0 & 1 & 0 & 0 \end{bmatrix} \tag{18}$$

## VI. EKF-UI Simulation results

In this section the results of the proposed EKF-UI are discussed. The EKF-UI for a biased SMA wire actuated robotic arm was tested through simulation using Matlab/Simulink environment. Noise was added to the system to emulate the system and measurements noise. For the system noise, changes in parameters like the damping coefficient of the joint and spring constant where made in the simulated model in comparison to the values used for the observer. In the case of the measurements noise, a Gaussian signal with zero mean was added to the position an velocity simulated vectors. Here the Gaussian signal variance was selected to emulate the average characteristics of commercial high resolution digital encoders. In Table I we can see the model parameters used for simulation.

TABLE I
PARAMETERS OF THE SMA WIRE AND THE COMPLIANT ACTUATOR [21], [22].

| Parameter | Value | Parameter | Value |
|---|---|---|---|
| $E_M$ | 28 $GPa$ | $C_A$ | 10 $Mpa/^oK$ |
| $E_A$ | 75 $GPa$ | $C_M$ | 10 $Mpa/^oK$ |
| $A_s$ | 88 $^oC$ | $T_{amb}$ | 25 $^oC$ |
| $A_f$ | 98 $^oC$ | $A$ | $4.9x10^{-8}$ $m^2$ |
| $M_s$ | 72 $^oC$ | $A_w$ | $290.45x10^{-6}$ $m^2$ |
| $M_f$ | 62 $^oC$ | $c_p$ | 320 $J/Kg^oC$ |
| $m_w$ | $6.8x10^{-4}$ $kg/m$ | $\varepsilon_L$ | 2.3% |
| $R$ | 20 $\Omega/m$ | $h_0$ | 20 |
| $l_0$ | 0.37 $m$ | $h_2$ | 0.001 |
| $b_s$ | 0.5 | $b_1, b_2$ | 0.1 |
| $k_s$ | 0.0018 $Nm/1^o$ | $\Theta$ | -0.055 |

The system was tested in open-loop with a sinusoidal input with an amplitude peak-peak of 6 V and a frequency of $1/60$ Hz. The results of this test are shown in Fig. 3, Fig. 4 and Fig. 5.

Figure 3 shows the tracking of the four states of the presented system. Here we can observe that all the states are accurately estimated using this approach, however, the angular velocity ($x_{2k}$) has a higher noise while being estimated. This is direct effect of derivating the position. Figure 4 shows the tracking error for the same four states. This figure shows that the convergence time for the estimated states is less than one second, except for the wire's temperature ($x_{3k}$) which takes around 15 seconds to converge. Despite the noise present on the estimation, the average estimation error is less than 0.05% for the temperature and 5% for the stress after convergence. We can see an increase in the error when the system crosses a transformation temperature (See Fig. 3 c) ), owing to the switching dynamics of the hysteretic system. Nonetheless, the observer is capable to converge again after a few seconds.

As mentioned before, the martensite fraction is an important parameter to model the behavior of a SMA wire, and a great alternative for control development. Nevertheless, it is a parameter difficult to measure in real applications since it depends on the microscopic internal transformation of the SMA wire. Our approach is capable of estimating this parameter as shown in Fig. 5 where the martensite fraction rate vs the estimated martensite fraction rate is plotted. Although some noise is shown, the estimation follows the switching dynamic behavior of this internal state accurately.

## VII. Conclusions

This work presents an Extended Kalman Filter with sliding mode unknown input and state estimation for a light-weight robotic arm actuated by shape memory alloy wires. Using the constitutive model for the development of the EKF-UI, the martensite fraction rate is estimated as an unknown input avoiding the use of switching dynamics inside the observer's model.

The simulation results prove the effectiveness of the proposed observer to deal with the hysteretic behavior of the SMA wires. The future perspective of the current result is

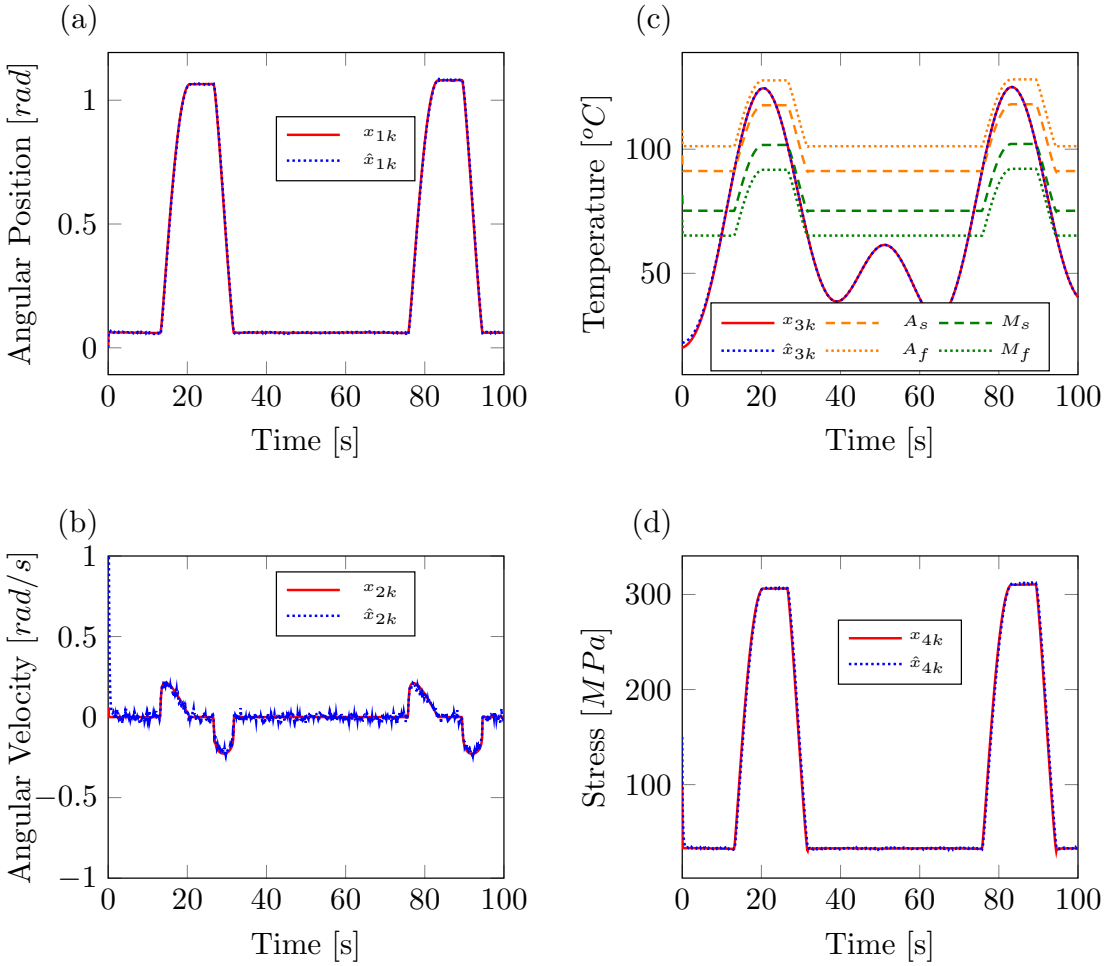


Fig. 3. Actual ($x_k$) vs EKF-UI estimated ($\hat{x}_k$) states , a) Angular position, b) Angular velocity, c) Wire's temperature, d) Wire's stress

to focus on the problem of noise reduction in the estimator and further perform control design using state feedback. Also as future work, the observer will be experimentally tested as the robotic arm's construction is completed.

## REFERENCES


[1] P. S. Lobo, J. Almeida, and L. Guerreiro, "Shape memory alloys behaviour: A review," *Procedia Engineering*, vol. 114, pp. 776 – 783, 2015, iCSI 2015 The 1st International Conference on Structural Integrity Funchal, Madeira, Portugal 1st to 4th September, 2015.

[2] J. Colorado, A. Barrientos, and C. Rossi, "Músculos inteligentes en robots biológicamente inspirados: Modelado, control y actuación," *Revista Iberoamericana de Automática e Informática Industrial RIAI*, vol. 8, no. 4, pp. 385 – 396, 2011.

[3] F. Nematzadeh and S. Sadrnezhaad, "Effects of material properties on mechanical performance of nitinol stent designed for femoral artery: Finite element analysis," *Scientia Iranica*, vol. 19, no. 6, pp. 1564 – 1571, 2012.

[4] H. Rodrigue, S. Cho, M.-W. Han, B. Bhandari, J.-E. Shim, and S.-H. Ahn, "Effect of twist morphing wing segment on aerodynamic performance of uav," *Journal of Mechanical Science and Technology*, vol. 30, no. 1, pp. 229–236, 2016.

[5] H.-M. Son, M. Y. Kim, and Y.-J. Lee, "Tunable-focus liquid lens system controlled by antagonistic winding-type sma actuator," *Optics Express*, vol. 17, no. 16, pp. 14 339–14 350, jul 2009.

[6] S. Quintanar-Guzmán, J. Reyes-Reyes, and M. d. c. Arellano-Sánchez, "Modelado y control de un sistema electrotérmico-mecánico móvil basado en alambres musculares," in *XVI Congreso Latinoamericano de Control Automático, CLCA 2014*. Asociación de México de Control Automático, 2014, pp. 834–839.

[7] S. Quintanar-Guzmán, S. Kannan, M. A. Olivares-Mendez, and H. Voos, "Operational space control of a lightweight robotic arm actuated by shape memory alloy (sma) wires," in *ASME 2016 Conference on Smart Materials, Adaptive Structures and Intelligent Systems*, vol. Volume 2: Modeling, Simulation and Control; Bio-Inspired Smart Materials and Systems; Energy Harvesting. Stowe, Vermont: American Society of Mechanical Engineers, 2016.

[8] R. Yousefian, M. A. Kia, and M. H. Zadeh, "Sensorless resistive-based control of shape memory alloy actuators in locking mechanism," *Journal of Intelligent Material Systems and Structures*, vol. 26, no. 4, pp. 450–462, 2015.

[9] J. H. Wiest and G. D. Buckner, "Indirect intelligent sliding mode control of antagonistic shape memory alloy actuators using hysteretic recurrent neural networks," *IEEE Transactions on Control Systems Technology*, vol. 22, no. 3, pp. 921–929, May 2014.

[10] A. Ianagui and E. A. Tannuri, "A sliding mode torque and position controller for an antagonistic SMA actuator," *Mechatronics*, vol. 30, pp. 126–139, 2015.

[11] H. Gurung and A. Banerjee, "Self-sensing SMA Actuator Using Extended Kalman Filter and Artificial Neural Network," *Procedia Engineering*, vol. 144, pp. 629–634, 2016.

[12] I. Hassanzadeh, N. Nikdel, and N. Motlagh, "Design of Augmented Ekf for Shape Memory Alloy Actuated Manipulator," *International Journal of Engineering Science and Technology*, vol. 2, no. 7, pp. 3188–3198, 2010.

[13] S. Jabeen, A. V. Yeganeh, G. M. Simsek, G. G. Yapici, K. Abidi, and O. Bebek, "Discrete-Time Integral Sliding Mode Control of a

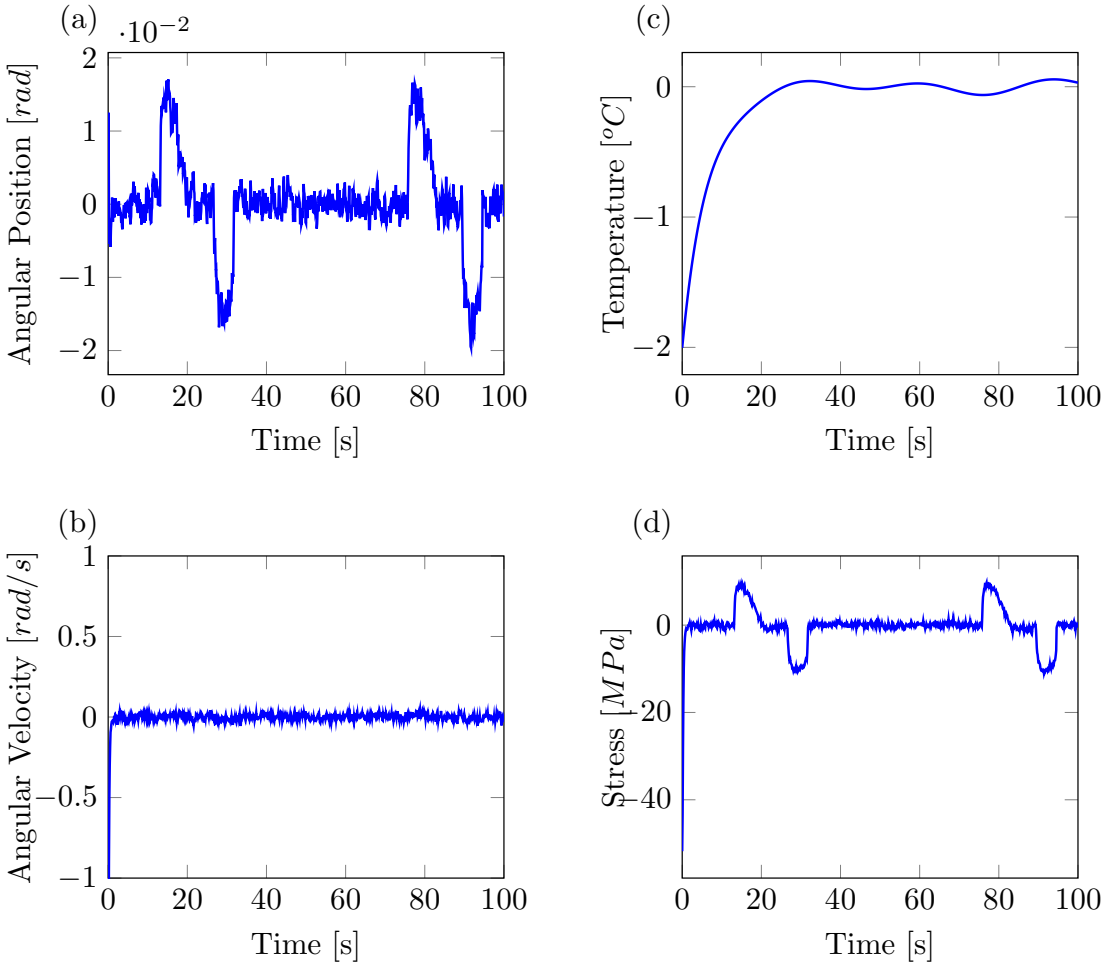


Fig. 4. Estimation error ($e = x_k - \hat{x}_k$) , a) Angular position error, b) Angular velocity error, c) Wire's temperature error, d) Wire's stress error

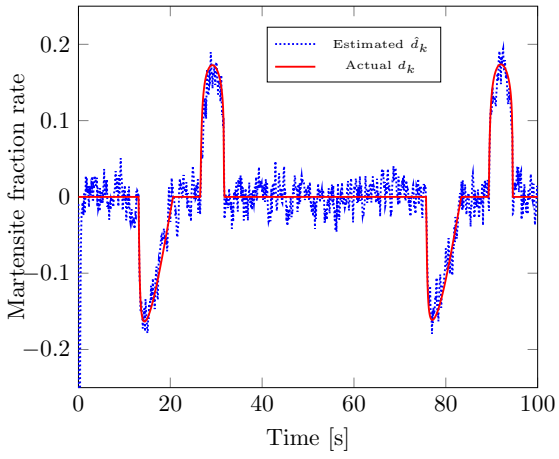


Fig. 5. Martensite fraction rate ($d_k$) vs estimated martensite fraction rate ($u_{rk}$) with EKF-UI (Unknown input).


Smart Joint for Minimally Invasive Surgeries," *6th IEEE RAS/EMBS International Conference on Biomedical Robotics and Biomechatronics (BioRob)*, 2016.

[14] S. Quintanar Guzmán, S. Kannan, M. A. Olivares Mendez, and H. Voos, "Lightweight robotic arm actuated by Shape Memory Alloy (SMA) Wires," in *International Conference on Electronics, Computers and Artificial Intelligence*, Ploiesti, Romania, 2016.

[15] Z. Guo, Y. Pan, L. B. Wee, and H. Yu, "Design and control of a novel compliant differential shape memory alloy actuator," *Sensors and Actuators A: Physical*, vol. 225, pp. 71–80, apr 2015.

[16] C. Liang and C. A. Rogers, "One-dimensional thermomechanical constitutive relations for shape memory materials," *Journal of intelligent material systems and structures*, vol. 1, no. 2, pp. 207–234, 1990.

[17] M. H. Elahinia and H. Ashrafiuon, "Nonlinear control of a shape memory alloy actuated manipulator," *Journal of Vibration and Acoustics*, vol. 124, no. 4, pp. 566–575, 2002.

[18] S. Quintanar-Guzmn, S. Kannan, A. Aguilera-Gonzlez, M. A. Olivares-Mendez, and H. Voos, "Operational space control of a lightweight robotic arm actuated by shape memory alloy wires: A comparative study," *Journal of Intelligent Material Systems and Structures*, in press.

[19] K. C. Veluvolu and S. Y. Chai, "High gain observers with multiple sliding mode for state and unknown input estimations," *2009 4th IEEE Conference on Industrial Electronics and Applications, ICIEA 2009*, vol. 56, no. 9, pp. 1179–1186, 2009.

[20] A. Aguilera-González, H. Voos, and M. Darouach, "States and unknown input estimation via non-linear sliding mode high-gain observers for a glucose-insulin system," in *2016 IEEE EMBS Conference on Biomedical Engineering and Sciences (IECBES)*, Dec 2016, pp. 388–393.

[21] . DYNALLOY Inc, "Flexinol actuator wire technical and design data," Available at: http://www.dynalloy.com/tech_data_wire.php, 2014, (accessed 26 April 2016).

[22] ——, "Technical characteristics of flexinol," Available at: http://www.dynalloy.com/pdfs/TCF1140.pdf, 2014, (accessed 26 April 2016).